Interplay between structure and magnetism in the spin-chain compound $(Cu,Zn)_2V_2O_7$

J. Pommer,[1] V. Kataev,[2,3] K.-Y. Choi,[1] P. Lemmens,[1,*] A. Ionescu,[1] Yu. Pashkevich,[4] A. Freimuth,[2] and G. Güntherodt[1]
[1]*II. Physikalisches Institut, RWTH Aachen, D-52056 Aachen, Germany*
[2]*II. Physikalisches Institut, Universität zu Köln, D-50937 Köln, Germany*
[3]*Kazan Physical Technical Institute, Russian Academy of Sciences, 420111 Kazan, Russia*
[4]*Donetsk Phystech NASU, 83114 Donetsk, Ukraine*

(Received 6 September 2002; revised manuscript received 31 January 2003; published 9 June 2003)

The structural and magnetic properties of the one-dimensional spin-chain compound $Cu_{2-y}Zn_yV_2O_7$ were investigated by means of x-ray diffraction, static susceptibility, and electron spin resonance. The substitution of nonmagnetic Zn^{2+} for Cu^{2+} ions induces a polymorphic transition from the α phase, found for $y<0.15$, to the β phase, which occurs for $y\geqslant 0.15$. This transition has a pronounced influence on the magnetic properties, which can be understood consistently by assuming that the intrachain Dzyaloshinsky-Moriya interaction is present in the α phase, but absent in the β phase. This interpretation is confirmed by a symmetry analysis of the structural and magnetic properties. Our results indicate that the local coordination geometry of Cu in the two phases is decisive for the magnetic properties.

DOI: 10.1103/PhysRevB.67.214410 PACS number(s): 71.27.+a, 75.30.Et, 76.30.Fc

I. INTRODUCTION

Experimental studies of low-dimensional spin systems aimed at testing fundamental theories of quantum magnetism have attracted much attention recently. A number of fascinating phenomena related to spin and charge correlations in one dimension were found, such as spin- and charge-density waves and spin-charge separation in organic charge-transfer salts,[1,2] the spin-Peierls transition in $CuGeO_3$,[3] and superconductivity in a Cu-based spin ladder compound.[4,5] Among inorganic materials, copper- and vanadium-based oxides with one hole (Cu^{2+}; $3d^9$) or one electron (V^{4+}; $3d^1$) in the *d*-shell often realize structurally well-defined quasi-one-dimensional (1D) spin 1/2 chains, in which the transition metal ions are bridged by oxygen ligands. The magnetic interactions in the chain are described using the Hamiltonian

$$\mathcal{H}=J\sum_{ij}\ \mathbf{S}_i\cdot\mathbf{S}_j+\sum_{ij}\ \mathbf{D}_{ij}[\mathbf{S}_i\times\mathbf{S}_j]+\sum_{ij}\ \mathbf{S}_iA_{ij}\mathbf{S}_j, \qquad (1)$$

where the first term represents the isotropic Heisenberg superexchange and the second and third terms denote the antisymmetric Dzyaloshinsky-Moriya (DM) and symmetric anisotropic corrections, respectively, which arise from spin-orbit coupling.[6,7] The sum in Eq. (1) runs over all pairs of nearest-neighbor spins. Since the orbital momentum in Cu^{2+} and V^{4+} oxides is almost completely quenched, the corrections due to spin-orbit coupling are small and the first term in Eq. (1) dominates. Thus, a one-dimensional-(1D-)Heisenberg isotropic $S=1/2$ chain can be closely realized in these compounds.

The magnitude and the sign of the exchange constant *J* are determined by the bonding geometry, according to the Goodenough-Kanamori-Anderson rules.[8] Although the spin-spin correlations decay very slowly along the chain, owing to quantum fluctuations true long-range order is impossible in one dimension even at $T=0$. However, the corrections to the isotropic Heisenberg superexchange given in Eq. (1) as well as the interchain interaction and interactions with the lattice and charge degrees of freedom may stabilize either a nonmagnetic spin-singlet state or 3D long-range order. In the latter case the DM interaction D_{ij}, if allowed by symmetry, is the strongest anisotropic correction to the Heisenberg superexchange. It is of first order in the spin-orbit coupling and may be comparable to the interchain interaction. The DM interaction leads to a canting of the spins, which often results in weak ferromagnetism in the magnetically ordered state. In addition, the DM interaction in low symmetry magnets renormalizes the magnetic anisotropy therefore affecting the choice of an ''easy'' axis.[9] Remarkably, if only the single-bond anisotropic superexchange interaction is considered, i.e., the interaction between only two neighboring spins, the anisotropies owing to the second and the third terms of Eq. (1) compensate each other exactly.[10] The combined effect of the DM and interchain interactions may cause unconventional phenomena such as the two-stage spin-flop transition reported for $BaCu_2Si_2O_7$.[11] The symmetric anisotropic part of the superexchange [third term in Eq. (1)] is of second order in the spin-orbit coupling, and therefore weaker than the antisymmetric DM interaction. Nevertheless, in Cu-based chain systems, for certain bonding geometries, also symmetric anisotropic corrections to superexchange may become surprisingly large.[12–15] Thus, the particular magnetic ground state of crystallographically quasi-1D transition metal oxides is sensitive to details of the crystal structure.

Copper-divanadate $Cu_2V_2O_7$, by virtue of its crystal structure, realizes an antiferromagnetic (AF) spin 1/2 chain. The magnetic moments in this compound arise solely from the Cu^{2+} cations, which are in a $3d^9$ configuration with $S=1/2$. The V^{5+} ions are nonmagnetic. The material crystallizes in two different phases, the low-temperature α phase[16,17] and the high-temperature β phase.[18] The structural phase transition occurs at 712 °C.[19,20] The α phase is orthorhombic (space group $Fdd2$) with lattice parameters $a=20.645$ Å, $b=8.383$ Å, and $c=6.442$ Å.[17] Each Cu ion is surrounded by five oxygen atoms, forming CuO_5 polyhedra (Fig. 1). The chains made of CuO_5 polyhedra are separated by $(V_2O_7)^{4-}$-anion groups, consisting of corner-sharing

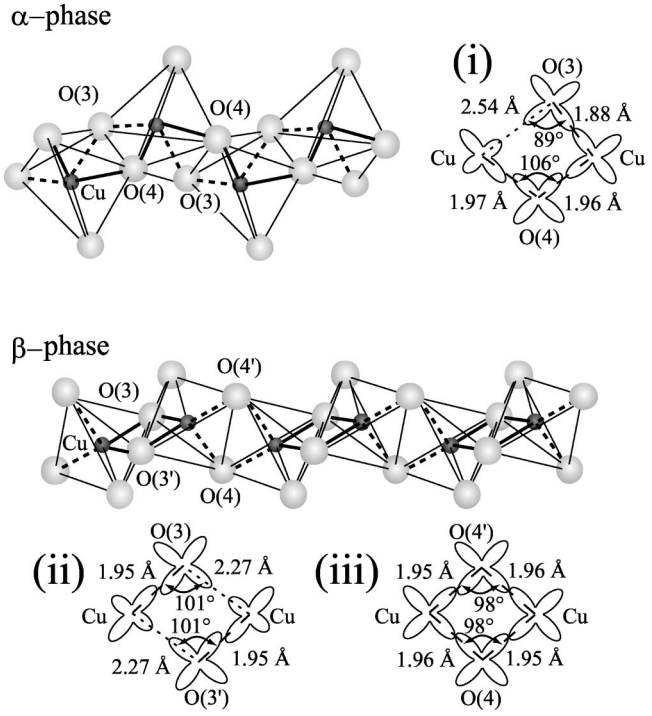

FIG. 1. Chains of CuO_5 polyhedra in the α and β phase. Bold solid and bold dashed lines denote inequivalent Cu-O-Cu bonds. The possible geometries of the Cu-O-Cu bonds (Ref. 20) as well as the sketch of the projections of the $d_{x^2-y^2}$ orbitals of Cu and p orbitals of O on the CuO_2 plaquettes are shown in (i), (ii), and (iii), respectively (see text).

VO_4 tetrahedra. The high-temperature β phase is monoclinic (space group $C2/c$) with lattice parameters $a=7.718$ Å, $b=8.044$ Å, $c=10.140$ Å, and $\beta=110.3°$.[20] The Cu^{2+} cations have again a fivefold oxygen coordination. The β phase is obtained from the α phase by rotating the V_2O_7 groups and shifting the planes of VO_4 tetrahedra.[17] In both structures the copper and vanadium atoms occupy only one crystallographic site, respectively. In spite of the overall structural similarity, the local Cu-O topology in the two phases is considerably different, as will be described in Sec. IV A. Measurements of the static magnetization in the α phase were reported in Ref. 21. Although the interaction between the Cu spins is antiferromagnetic, a spontaneous magnetization is observed below 35 K with a small saturation magnetization of $0.04\mu_B$. This suggests a state with long-range AF order and weak ferromagnetism, arising from a canting of spins due to the DM interaction.[21]

We report in this paper on an interplay between structure and magnetism in $Cu_{2-y}Zn_yV_2O_7$ which was studied by means of static susceptibility, electron spin resonance (ESR) and x-ray diffraction. A moderate substitution of nonmagnetic Zn for Cu causes a drastic change of the magnetic properties, occurring at $y\simeq 0.15$, which is accompanied by a polymorphic transition from the α to β phase. We provide a consistent interpretation of such a strong impact of the structural transition on the magnetic properties assuming that the intrachain Dzyaloshinsky-Moriya interaction is present in the α phase, but absent in the β phase. This scenario is justified by a symmetry analysis of magnetic interactions in the two structural phases. Our results indicate that the local coordination geometry of Cu in the two phases is decisive for the magnetic properties.

II. EXPERIMENTAL DETAILS

Polycrystalline samples of $(Cu,Zn)_2V_2O_7$ were prepared by a solid-state reaction from oxides. The respective amount of CuO, ZnO, and V_2O_5 were ground and, using gold crucibles, homogenized at a temperature of 530 °C in air for eight hours, and subsequently fired in air for twenty hours. Firing and grinding were repeated until small crystallites were obtained. Finally, the powders were sintered at 650 °C in air for 110 h. Note that this temperature is lower than the melting point of 780 °C and the structural phase transition temperature of 712 °C.[19,20]

The samples were characterized by powder x-ray diffraction using CuK_α radiation. The raw data were analyzed with the crystallographic program CARINE. Peaks with less than 5% of the intensity of the main peak were neglected. The static susceptibility (χ) and the magnetization (M) were measured with a superconducting quantum interference device (SQUID) magnetometer for temperatures T ranging between 2 and 300 K. ESR measurements were carried out using a Bruker spectrometer at X-band frequency 9.48 GHz. A continuous flow He cryostat inserted into the microwave cavity enabled us to measure the ESR signal for $2\ \mathrm{K}<T<300$ K. To obtain the ESR intensity in absolute units the intensity of the measured signal was calibrated using a ''witness'' sample ($Al_2O_3+0.03\%\ Cr^{3+}$), which was attached to the wall inside the cavity.

III. RESULTS

A. Static magnetic susceptibility

Our results on the magnetic susceptibility $\chi(T)$ of $Cu_{2-y}Zn_yV_2O_7$ measured in a magnetic field $H=1$ T are summarized in Fig. 2. $\chi(T)$ follows the Curie-Weiss law $\chi_{CW}=C_{mol}/(T-\Theta)$ over a wide temperature range. Here, C_{mol} is the molar Curie constant and Θ is the Curie-Weiss temperature. As a representative example, a fit to the Curie-Weiss law is shown for $Cu_2V_2O_7$ in the inset of Fig. 2. The fit yields $\Theta=-78$ K and an effective moment $\mu_{eff}=\sqrt{3k_BC_{mol}/N_A}\approx 1.9\mu_B$. Here k_B is the Boltzmann constant, N_A is the Avogadro number, and μ_B is the Bohr magneton. As expected theoretically, μ_{eff} is slightly larger than the spin-only value of $\mu=g\mu_B\sqrt{S(S+1)}=1.73\mu_B$ for $S=1/2$ and a g factor $g=2$. This discrepancy indicates that μ_{eff} contains a small admixture of the orbital moment, as is typical for Cu^{2+}. Assuming that Θ is determined by the strongest nearest-neighbor exchange coupling J yields $\Theta=-zJS(S+1)/3k_B$ in molecular field approximation. Here z is the number of nearest neighbors. If only the intrachain coupling is taken into account, $z=2$, we obtain an AF exchange interaction between nearest-neighbor Cu ions of $J=155$ K. This value should be considered as an order of

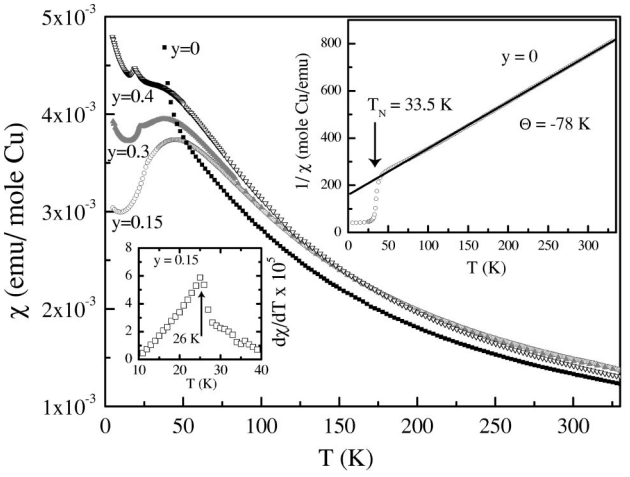

FIG. 2. Temperature dependence of the static magnetic susceptibility of $Cu_{2-y}Zn_yV_2O_7$ measured at 1 T. Upper inset: χ^{-1} for $Cu_2V_2O_7$. The solid line is a fit to the Curie-Weiss law (see text.) Lower inset: $\partial\chi(T)/\partial T$ for the $y=0.15$ sample as a function of temperature. The jumplike anomaly indicates magnetic ordering at $T_N=26$ K.

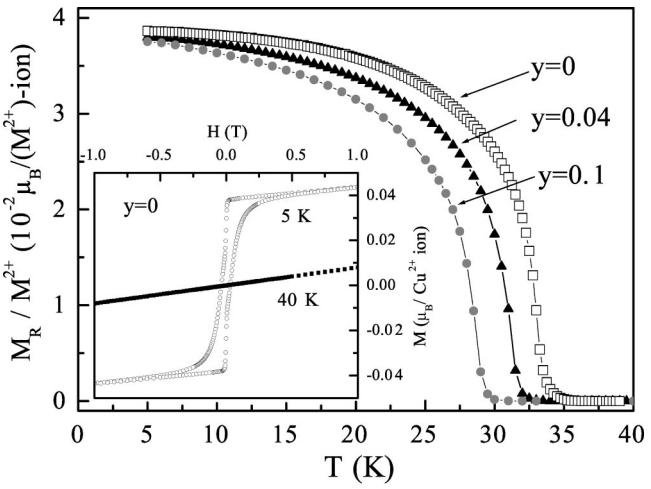

FIG. 3. Temperature dependence of the remanent magnetization M_R of $Cu_{2-y}Zn_yV_2O_7$ for $0\leqslant x\leqslant 0.1$. M_R was measured in zero field after applying an external field of 1 T at a temperature $T=5$ K. M^{2+} stands for the Cu and Zn ions. Inset: Hysteresis of the magnetization for $Cu_2V_2O_7$ at 5 and 40 K.

magnitude estimate only, as the considerable interchain interactions (see below) contribute to Θ as well. According to the Goodenough-Kanamori-Anderson rules the moderate AF coupling along the chains indicates a relatively small deviation of the Cu-O-Cu bonding angle from 90° (see Sec. IV A below); for larger deviations one would expect a much larger value of J, as found, e.g., in the 2D cuprates, where $J\approx 1500$ K for 180° Cu-O-Cu bonds.[22]

The static susceptibility of $Cu_2V_2O_7$ shows an abrupt strong increase at $T=34$ K, indicating a transition to a magnetically ordered state (Fig. 2). Below 34 K a small remanent magnetization M_R occurs and we find hysteresis in the field dependence of the magnetization $M(H)$ (see Fig. 3). The leading isotropic exchange interaction J is antiferromagnetic and the saturation magnetization of $0.04\mu_B$ is small compared to $1\mu_B$, which would correspond to ferromagnetically ordered $S=1/2$ spins. We therefore conclude that $Cu_2V_2O_7$ is a canted antiferromagnet with an ordering temperature of $T_N=33.5$ K. This conclusion is consistent with the data reported in Ref. 21. Canting of spins in an antiferromagnet and the associated weak ferromagnetism are a fingerprint of the DM interaction. Using $M_R(0)=0.04\mu_B/Cu^{2+}$ we estimate the canting angle of the AF sublattice magnetization as $\phi_{DM}\simeq\tan\phi_{DM}=M_R(0)/g\mu_BS=D_{ij}/2J\approx 2°$.[7] This gives the magnitude of the DM interaction D_{ij} in Eq. (1), which amounts to $\sim 7\%$ of the isotropic coupling constant J. We note that because $M_R(0)$ obtained from a powder measurement is an average of the saturation magnetization over all orientations the actual canting angle and the magnitude of the DM interaction might be even larger.

Substitution of nonmagnetic Zn for Cu in $Cu_{2-y}Zn_yV_2O_7$ up to $y=0.1$ leads to a decrease of T_N (see Fig. 5), as expected, owing to an increase of the mean distance between the spins and a respective decrease of the effective average magnetic exchange. The remanent magnetization M_R, however, remains constant with increasing Zn content y. Remarkably, for $y>0.15$ the static magnetic properties change drastically: Instead of the steep upturn at low temperatures, $\chi(T)$ shows a broad maximum at a temperature $T_{max}\simeq 45$ K (Figs. 2 and 4); moreover, the remanent magnetization and the hysteresis of $M(H)$ disappear. A transition to an ordered state can, nevertheless, be clearly identified from the discontinuous jump at T_N in the derivative $d\chi(T)/dT$ of the static susceptibility (inset of Fig. 2). With increasing y a Curie-like tail in $\chi(T)$ develops at low T, so that at $y=0.4$ the broad maximum of $\chi(T)$ transforms into a plateau (Fig. 2).

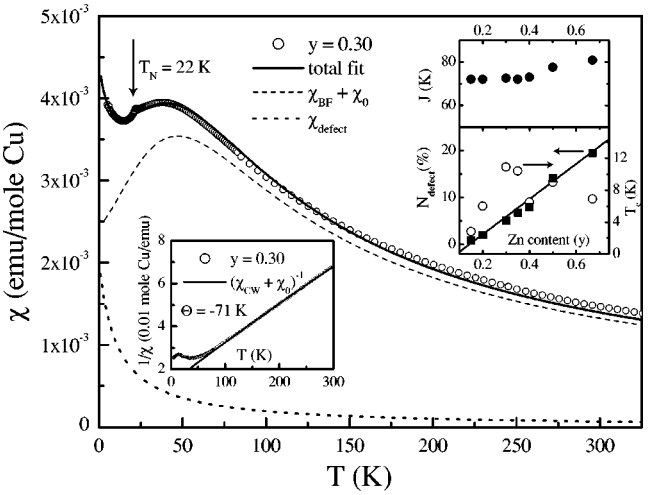

FIG. 4. Temperature dependence of the static magnetic susceptibility $\chi(T)$ of $Cu_{2-y}Zn_yV_2O_7$ for $y=0.30$. The solid, dashed, and dotted lines are the total fitting function [Eq. (2)] and different contributions to it, respectively (see text). Upper inset: Fit parameters [Eq. (2)] as a function of Zn concentration. Lower inset: Temperature dependence of $\chi^{-1}(T)$ with a fit to the Curie-Weiss law (solid line).

The susceptibility of the samples with $y \geqslant 0.15$ with the broad maximum at $T_{max} > T_N$ is reminiscent of that of a 1D-Heisenberg antiferromagnet where the temperature of the maximum T_{max} and the height of the maximum χ_{max} are related to the nearest-neighbor intrachain exchange constant J as $T_{max} = 0.641 J/k_B$ and $\chi_{max} = 0.147 N g^2 \mu_B^2 / J$, respectively.[23] In fact, the temperature evolution of χ can be reasonably well described as a sum of three contributions

$$\chi(T) = \chi_0 + \chi_{BF}(T) + \chi_{defect}(T), \tag{2}$$

where the temperature independent χ_0 is a sum of the diamagnetic susceptibility of $Cu_{2-y}Zn_yV_2O_7$ and the Van-Vleck susceptibility of Cu^{2+}, $\chi_{BF}(T)$ is the Bonner-Fisher susceptibility of a 1D-antiferromagnetic spin chain[23,24] and $\chi_{defect}(T) = N_{defect} g^2 S(S+1) \mu_B^2 / 3k_B (T - T_c)$ is the Curie-Weiss susceptibility of the ''defect'' magnetic sites which contribute to the low-T upturn of $\chi(T)$. As a representative example we show in Fig. 4 the result of the fit of Eq. (2) to the susceptibility of the $y = 0.30$ sample. The height and the position of the maximum of $\chi(T)$ is reproduced well with $J = 72$ K and $g = 2.13$ (see Sec. III B). The fit requires a value of $\chi_0 = 1 \times 10^{-4}$ emu/mole which is kept constant for all samples. The strength of the AF intrachain exchange does not depend on the Zn concentration up to $y = 0.40$ and then slightly increases, whereas the concentration of the defect spins N_{defect} and their T_c grow rapidly with increasing y as shown in the upper inset of Fig. 4. In particular N_{defect} increases almost linearly with y suggesting that each Zn atom creates ~ 0.8 spins $S = 1/2$. The occurrence of quasifree magnetic moments is a remarkable feature of the hole-doped two-dimensional high-T_c cuprates where the removal of one spin form the AF spin-liquid background generates an uncorrelated spin localized around the vacancy (see, e.g., Ref. 25). A systematic increase of the Curie-like tail in the susceptibility of $Cu_{2-y}Zn_yV_2O_7$ with $y \geqslant 0.15$ implies that nonmagnetic Zn substitution for Cu creates apparently similar defect sites in the spin chain as well.[26]

At sufficiently high temperature, above T_{max}, $\chi(T)$ follows the Curie-Weiss law reasonably well, with values of Θ of the same order of magnitude as in the samples with Zn content $y < 0.15$ (Ref. 27) (lower inset of Fig. 4). After an abrupt but moderate increase around $y = 0.15$, Θ continues to decrease with y, indicating a further weakening of the effective average magnetic exchange due to the dilution of spins (Fig. 5). The ordering temperature T_N decreases with increasing the concentration of nonmagnetic Zn as well. Notably, T_{max} is only twice as large as T_N. This may indicate significant interchain coupling and anisotropic spin-spin interactions which drive the system into the magnetically ordered state.[28] The strength of the interchain coupling J_{inter} can be estimated in the mean-field approximation as $J_{inter} = T_N / 1.28\sqrt{\ln(5.8J/T_N)}$.[29] With $J = 72$ K and $T_N = 26$ K we obtain $J_{inter} \simeq 12$ K, which is only 6 times smaller than J. In the renormalized spin wave theory one obtains a somewhat smaller result of $J_{inter} \simeq 8$ K.[30,31] Remarkably the ordering temperature T_N changes smoothly across the Zn concentration $y = 0.15$, whereas Θ, a measure of the average magnetic exchange, increases at this point appreciably. This may indicate that the ratio J/J_{inter} for the samples with $y < 0.15$ is even smaller than that for the samples with $y \geqslant 0.15$. It may be the reason why the susceptibility of $Cu_{2-y}Zn_yV_2O_7$ with $y < 0.15$ does not show features of 1D antiferromagnetism and follows closely the Curie-Weiss law down to T_N. Since T_N is more sensitive to the changes of J_{inter}, an appreciable increase of J may be compensated by a relatively small decrease of J_{inter} to keep T_N constant.

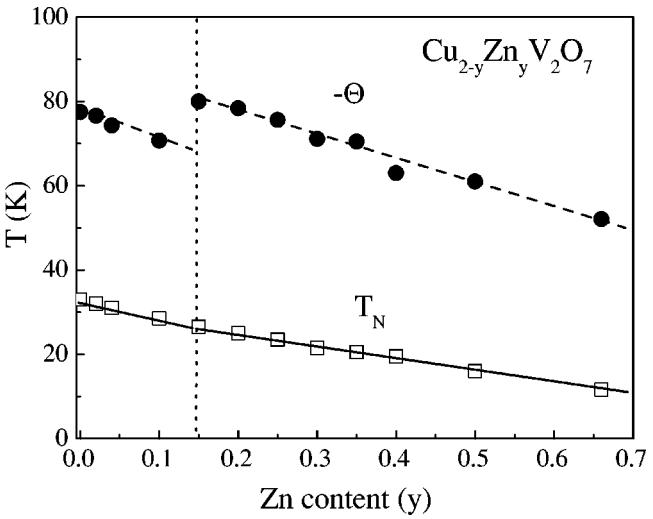

FIG. 5. Curie-Weiss constant Θ and Néel temperature T_N as a function of Zn content y. Note the discontinuous behavior close to $y = 0.15$. The solid and dotted lines are a guide to the eye.

B. Electron spin resonance

ESR spectra of $Cu_2V_2O_7$ at selected temperatures are shown in Figs. 6(a) and 6(b). The weak signals in the field range 2–4 kOe occurring above about 22 K can be presumably attributed to a small amount of impurities or structural defects. No resonant absorption due to bulk Cu spins is detected. Below 22 K a strong signal develops at low fields, with an intensity increasing with decreasing temperature [Fig. 6(b)]. This low-field absorption line, which is present only below T_N, can be considered as a signature of weak ferromagnetism.[32,33] It is not expected for an AF spin lattice of rhombic or lower symmetry without spin canting. In this case only the ''hard'' AF mode should occur at a microwave frequency well above the X-band frequency.[9]

The Zn-doped samples with $y = 0.2$ and $y = 0.4$ show a strong ESR signal in a wide temperature range. A typical spectrum is shown in Fig. 6(c). The shape of the spectrum is described well by the derivative of a Lorentzian absorption line. The intensity of the signal is determined by the static susceptibility χ^{ESR} of the spins participating in the resonance.[34] χ^{ESR} can be obtained from a comparison with the ESR signal of the standard reference sample with known ESR spin susceptibility. Although the determination of the absolute value of the spin susceptibility from ESR suffers from a number of uncertainties, the value of χ^{ESR} at room temperature obtained in this way differs only by $\sim 10\%$ from that obtained from the SQUID measurements. With the exception of the temperature region near T_N (see below), also

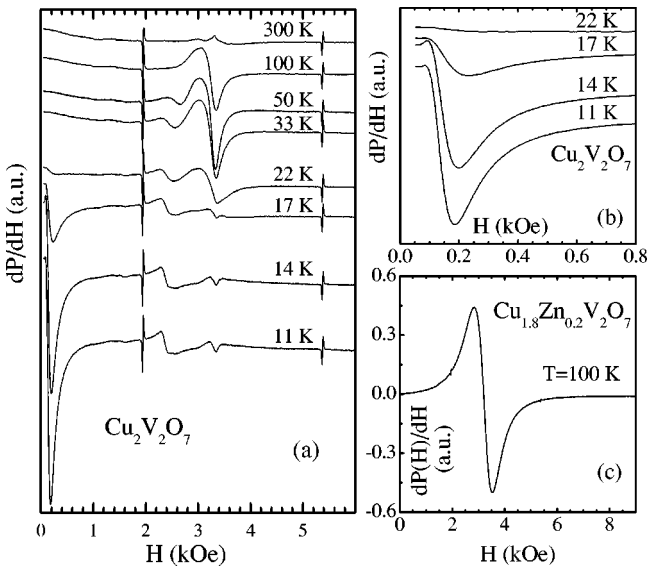

FIG. 6. ESR spectra of $Cu_{2-y}Zn_yV_2O_7$. dP/dH is the derivative of the absorbed microwave power. Narrow resonances at ~ 2000 and ~ 5400 Oe correspond to the reference sample. (a) ESR spectra of the $y=0$ sample at selected temperatures. Note the strong signal at low fields for $T \leqslant 22$ K which is shown in (b) on an expanded scale. (c) ESR spectrum of the $y=0.20$ sample at $T=100$ K.

the temperature dependence of χ^{ESR} normalized at $T=300$ K is consistent with that of the static susceptibility (Fig. 7), suggesting that ESR and the static magnetic susceptibility probe the same Cu^{2+} spins.

The resonance field H_{res} as a function of temperature is plotted in Fig. 7. It is almost temperature independent above about 30 K, but increases strongly with decreasing temperature at lower temperatures. The g factor obtained from $g=h\nu/\mu_B H_{\mathrm{res}}$ is shown in the same figure. Here h is the Planck constant and ν is the ESR frequency. Due to spin-orbit coupling and the low symmetry of the crystal field associated with the CuO_5 polyhedron the g factor of a Cu^{2+} ion should be anisotropic, and the powder spectrum yields only an average g factor. Since the shape of the powder signal is described by a single Lorentzian profile, the anisotropy of the g factor for a given sample is smaller than the width of the line ΔH. With $\Delta H(T=300\ \mathrm{K}) \approx 900$ Oe one expects that it is less than $\approx 10\%$ of the mean value of g. We find $g_{\mathrm{mean}}=2.12$ and 2.135 for $y=0.2$ and 0.4, respectively.[35] The dependence of the average g factor on y suggests that Zn substitution influences the steric parameters of a CuO_5 polyhedron and thus the crystal field potential at the Cu site (see Sec. III C).

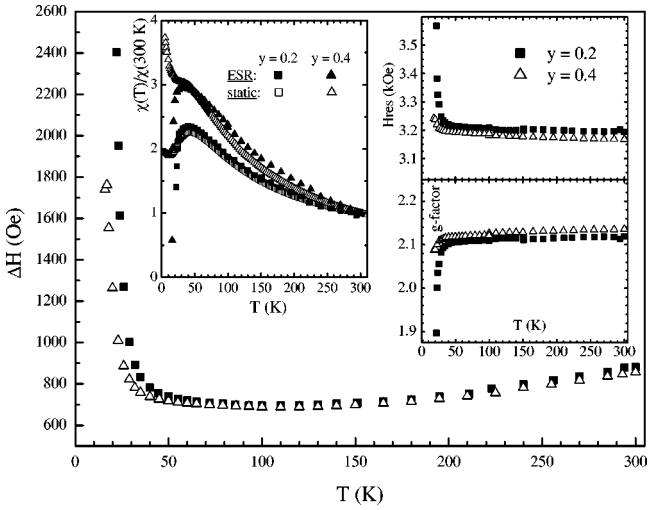

FIG. 7. Parameters of the ESR signal of $Cu_{2-y}Zn_yV_2O_7$ ($y=0.2$ and 0.4). Main panel: temperature dependence of the ESR linewidth ΔH. Left inset: static susceptibility (open symbols) and spin susceptibility derived from the ESR intensity (full symbols) normalized at $T=300$ K. Right inset: temperature dependence of the resonance field H_{res} and of the g factor.

The temperature dependence of ΔH is shown in Fig. 7. Above about 50 K the data are independent of the Zn concentration within our experimental resolution. The behavior of ΔH above 50 K is typical for ESR of Cu^{2+} in concentrated paramagnetic insulators. The width ΔH is mainly determined by interactions between Cu spins which occupy regular lattice sites. In the high temperature limit, i.e. when $\chi(T)$ obeys the Curie law, ΔH due to spin-spin interactions does not depend on T. The slight increase of ΔH above 150 K may indicate an additional relaxation process via phonons. This effect is relatively small, because of the quenching of the orbital momentum of Cu^{2+} by the crystal field.

The drastic increase of ΔH in the low-temperature regime, which is accompanied by a strong shift of the resonance field (Fig. 7), indicates clearly the onset of short-range magnetic order. The critical behavior of ESR in the vicinity of the magnetic phase transition is caused by the fluctuations of the staggered magnetization in the AF correlated regions and by the development of the static internal field[36,37]. The former effect broadens the signal, whereas the latter shifts the resonance line.[38,39] The ESR intensity drops rapidly and the signal vanishes at T_N, as expected at this frequency for a low-symmetry antiferromagnet without spin canting.[9] In contrast to the undoped sample no ferromagneticlike absorption associated with weak ferromagnetism is observed in the AF state. Also the resonance of the quasifree spins which for $y \geqslant 0.4$ dominate the static magnetic response below T_N is not observed. The absence of this resonance signal can be understood assuming that these ''defect'' spins are subjected to strong internal fields in the AF ordered lattice and their resonance frequencies are therefore out of the range of our spectrometer. The critical behavior of ESR weakens with increasing Zn concentration, which can be attributed to spin dilution, consistent with the data from the static magnetic suceptibility.

C. X-ray diffraction

The dilution of the spins with increasing Zn doping is unlikely to produce the drastic, qualitative change of the magnetic properties found at $y=0.15$. One may therefore suspect that Zn defects influence the magnetic properties indirectly, e.g., via a distortion of the lattice. This is verified by our x-ray diffraction studies. Two $\Theta/2\Theta$ scans representative

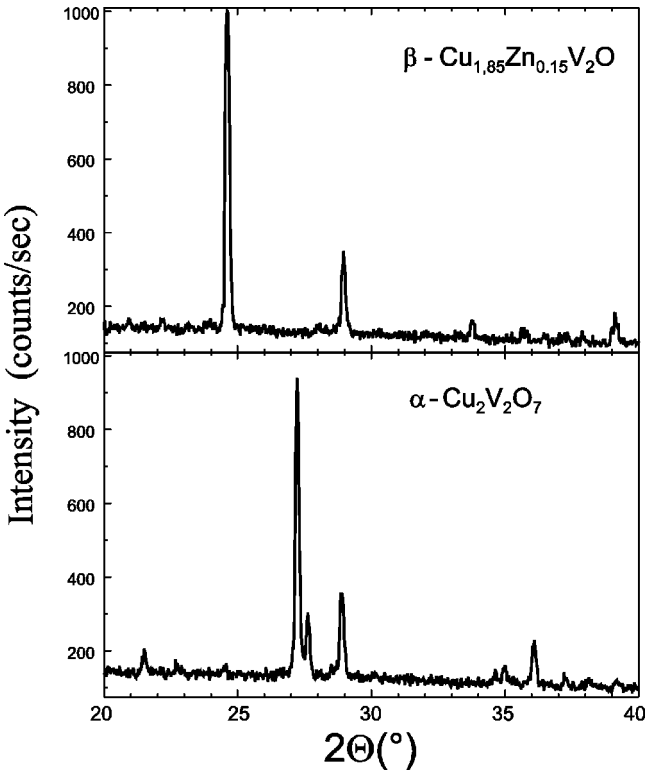

FIG. 8. X-ray diffraction patterns of $y=0$ and $y=0.15$ samples.

for samples from the low ($y<0.15$) and high ($y\geqslant 0.15$) doping regimes of the magnetic phase diagram are shown in Fig. 8. These diffraction patterns are clearly different. The pattern for $y=0$ is identified with that of the α phase, and that of $y=0.15$ with the β phase of $Cu_2V_2O_7$ (Fig. 1).

Crystallographic characterization of a series of $Cu_{2-y}Zn_yV_2O_7$ solid solutions was reported in Ref. 40. The β phase is found for $0.25\leqslant y\leqslant 2$. The samples were synthesized at temperatures above the structural transition temperature of $Cu_2V_2O_7$, and then quenched. This would imply that the β phase could be metastable. However, the sintering temperature of our samples is smaller than the phase transition temperature, suggesting that the β phase in the doped samples is a thermodynamic equilibrium phase.

A possible cause for the $\alpha\rightarrow\beta$ transition is the shortening of the apical *M*-O bond and the lengthening of the equatorial bonds of MO_5 polyhedra ($M=$Zn ,Cu), which occurs with increasing the Zn concentration.[40] Because MO_5 polyhedra in the neighboring chains are linked by $(V_2O_7)^{4-}$-anion groups, the Zn-induced changes of the bond lengths of the former may cause reorientations of the latter required for the anion packing of the β phase.[16–18] As discussed in Ref. 40, CuO_5 polyhedra are elongated due to the Jahn-Teller effect. Zn^{2+} ion is, however, not Jahn-Teller active. Thus, ZnO_5 polyhedra have no internal driving mechanism for distortion, which explains the observed changes of the metal-ligand bond lengths with increasing substitution of Zn for Cu as well as the change of the *g* factor.

IV. DISCUSSION

A distinct feature of the magnetically ordered state of $(\underline{Cu},Zn)_2V_2O_7$ emerging from our study is the occurrence of weak ferromagnetism in the α phase and its absence in the β phase. Since weak ferromagnetism is usually associated with the DM interaction, this suggests that the DM interaction is allowed by symmetry in the α phase, but forbidden in the β phase. To analyze this in more detail, we first examine qualitatively the exchange paths between nearest-neighbor Cu^{2+} spins in the two phases. We then present a more detailed symmetry analysis of magnetic interactions which enables us to propose possible types of magnetic order and to discuss the relationship between the anisotropy of exchange and ESR.

A. Local bonding geometry

In the α phase each Cu atom is surrounded by five oxygen atoms forming distorted CuO_5 polyhedra (Fig. 1). CuO_5 complexes build up a network of mutually perpendicular chains along the [011] and the $[01\bar{1}]$ directions, where the shortest distance between Cu atoms is found. Thus we assume that the exchange interaction is dominated by paths along the chains. The nearest-neighbor (NN) Cu atoms in each chain are coupled by two asymmetric bonds Cu-O(3)-Cu and Cu-O(4)-Cu, respectively, forming a CuO_2 plaquette. The relevant bond lengths and bond angles are indicated in Fig. 1(i).[20] The projections on that plaquette of the $d_{x^2-y^2}$ orbitals of copper and $p_{x,y}$ orbitals of oxygen involved in the bonding are sketched in the same figure. Because the $d_{x^2-y^2}$ orbital of the left Cu is strongly inclined from the plaquette its overlap with the *p* orbital of O(3) is considerably smaller than with the *p* orbital of O(4). It is also smaller than the overlap of the right Cu $d_{x^2-y^2}$ orbital with O(3) and O(4) *p* orbitals. Furthermore, the distance between the left Cu and O(3) is the largest within the plaquette.

The pronounced asymmetry of the bonding implies the occurrence of two different paths for the NN magnetic exchange. According to the Goodenough-Kanamori-Anderson rules, the first path Cu-O(3)-Cu leads to a weak ferromagnetic interaction; the second one, Cu-O(4)-Cu, owing to the larger deviation of the bonding angle from 90° (Ref. 13) and the stronger overlap of the orbitals, causes a relatively strong AF interaction. The exchange constant *J* of order 100 K found from our data analysis can then be understood as the sum of two superexchange integrals. Thus, one may view the spin structure in α-$Cu_2V_2O_7$ as a network of zigzaglike AF chains of Cu^{2+} ions, which point alternately along the [011] and $[01\bar{1}]$ directions. To check for the presence of the DM interaction between the NN Cu spins we introduce the DM vector

$$\mathbf{D}_{ii+1}=D_0\cdot[\mathbf{n}_{io}\times\mathbf{n}_{oi+1}]. \tag{3}$$

Here $\mathbf{n}_{io}$ and $\mathbf{n}_{oi+1}$ are the space vectors connecting the neighboring Cu ions with the bridging oxygen. If the two bonds bridging the NN Cu sites were symmetric, the DM vectors of the respective exchange paths would have, according to Eq. (3), the same magnitude but point at the opposite directions, thus compensating each other. Since in the α phase the bonding geometry is, however, appreciably asym-

metric the two DM vectors arising from the two different exchange paths do not cancel each other, yielding the net DM interaction.

In the β phase the chains of CuO_5 polyhedra are formed along the [110] and [$1\bar{1}0$] directions (Fig. 1). Each Cu atom is coupled to its two neighbors in the chain via two inequivalent pairs of oxygens [O(3), O(3′)] and [O(4), O(4′)], respectively. Thus in the β phase two types of edge-sharing CuO_2 plaquettes with somewhat different geometry are present, as shown in Figs. 1(ii) and 1(iii), respectively. The projections on the plaquettes of the relevant $d_{x^2-y^2}$ orbitals of copper[41,42] and $p_{x,y}$ orbitals of oxygen are sketched in these figures as well. In the first geometry [Fig. 1(ii)] the $d_{x^2-y^2}$ orbitals are inclined from the plaquette so that the overlap of the orbitals between the left Cu and O(3′) and the right Cu and O(3) is weaker than in the left Cu-O(3) and the right Cu-O(3′) bonds, respectively. Also the bond lengths Cu-O(3′) and O(3)-Cu are the largest in the chain. In the second geometry [Fig. 1(iii)] the orbital overlap is larger and all bonds are of almost the same short length. Because of the difference of the steric parameters one therefore expects two constants of the NN exchange J and J' which alternate along the chain. However, it is feasible that the weaker overlap of the orbitals in the first CuO_2 plaquette is compensated by the larger Cu-O-Cu bond angle of 101°, as compared to 98° in the second plaquette, resulting in a rather small alteration of the exchange constant. In fact, a satisfactory description of the static susceptibility has been obtained with only one exchange constant, i.e., by assuming $J \approx J'$. Note that the DM vector is expected to vanish in the β-phase because the exchange paths bridging the NN Cu sites, e.g., Cu-O(3)-Cu and Cu-O(3′)-Cu, are symmetric. Thus, β-$Cu_2V_2O_7$ can be considered as a weakly alternating zigzaglike AF chain without DM interaction.

B. Symmetry analysis and possible types of magnetic order

The qualitative considerations in the previous section are confirmed by a more elaborate symmetry analysis following Bertaut[43] and Izyumov and Naish.[44] The details of this examination are given in Appendix A. The main conclusion which follows from the analysis of the transformation of spins under the symmetry operations of a crystallographic space group of the α and β phases of $(\underline{Cu},Zn)_2V_2O_7$ is that weak ferromagnetism is possible in the α phase only, whereas it is inconsistent with AF ordering of spins in the chains of the β phase.

The group theory analysis of the magnetic interactions between the Cu^{2+} spins given in Appendix A enables one to determine the orientation of a weak ferromagnetism vector as well as the possible types of magnetic ordering. For this purpose the Hamiltonian [Eq. (1)] can be rewritten in a more general form which includes also an interaction with a magnetic field:

$$\mathcal{H}=\sum_{i\alpha j\beta} K^{ij}_{\alpha\beta} S^i_\alpha S^j_\beta - \mu_B \sum_{ij\alpha} g^{ij}_\alpha H_i S^j_\alpha . \tag{4}$$

Here g^{ij}_α is the g-factor tensor of the αth ion, and $K^{ij}_{\alpha\beta} = \Sigma_m K^{ij}_{\alpha\beta}(n,m)$, where $K^{ij}_{\alpha\beta}(n,m)$ is the tensor of spin interactions between the α sublattice in the nth primitive cell and the β sublattice in the mth primitive cell. Because of permutation symmetry only four interactions, K^{ij}_{11}, K^{ij}_{12}, K^{ij}_{13}, and K^{ij}_{14} are independent. According to Moriya[7] the diagonal part of $K^{ij}_{\alpha\beta}$ can be decomposed into $K^{ii}_{\alpha\beta} = J_{\alpha\beta} + A^{ii}_{\alpha\beta}$, where $A^{ii}_{\alpha\beta}$ represents the anisotropy of exchange between the α and β sites along the i direction. The explicit form of the interaction tensors $K^{ij}_{\alpha\beta}$ obtained by the symmetry analysis and a discussion of their properties are given in Appendix B. Here we summarize the main conclusions. In the α phase the antisymmetric intrachain interaction gives rise to a DM vector which lies preferably in the yz plane. In the β phase the intrachain interaction is purely symmetric and the spin structure is incompatible with weak ferromagnetism. The arrangement of spins in the magnetic unit cell depends on the sign of the interchain exchange. The alignment of the AF vectors of the chains is parallel for the ferromagnetic sign and is antiparallel for the AF sign of the interchain coupling. Moreover, the interchain interaction plays an essential role by restoring three dimensionality. One expects that the increase of the shortest interchain distance between Cu ions from 4 Å in the α phase to 4.64 Å in the β phase[20] leads to a smaller value of the interchain coupling in the β phase, consistent with the results of the analysis of the susceptibility data in Sec. III A.

C. Anisotropy of exchange and electron spin resonance

The Hamiltonian [Eq. (4)] and the expressions [Eqs. (B2)–(B5)] allow also for a discussion of the effect of magnetic interactions between Cu^{2+} spins on the ESR spectrum. It is well known that the isotropic exchange narrows the ESR signal, whereas anisotropic contributions to the magnetic exchange broaden it.[34] In three-dimensional paramagnets in the high-temperature limit the resulting width of the ESR signal due to the spin-spin interactions can be estimated as[45]

$$\Delta H_{\rm ex} \approx \frac{1}{g\mu_B}\frac{M_2^2}{|J|}, \tag{5}$$

where the so-called second moment M_2 of the resonance line is given by the anisotropic corrections to the superexchange and $J=(1/2)J_{12}$, as defined in Eq. (B6). Owing to an appreciable interchain exchange coupling in $Cu_2V_2O_7$ of the order of 10 K (see Sec. III A) the rate of the out-of-chain diffusion of spin correlations set by this coupling[31] is much faster than the ESR frequency ($h\nu/k_B \sim 0.5$ K). Thus the spins behave essentially three dimensionally on the ESR time scale and Eq. (5) is applicable in this case.

The effect of the DM interaction on the ESR linewidth in 1D spin chains has been studied recently in Refs. 39,46, where it is claimed that the theory of exchange narrowing is inadequate for describing the DM effects. In particular, it is shown that the DM interaction gives the same contribution to ΔH as the symmetric anisotropy, although in the traditional literature the antisymmetric DM terms D are usually expected to give the largest contribution to ΔH because they are the first order spin-orbit perturbation, whereas the symmetric anisotropic terms d are the second order

corrections.[34,6,7] Apparently, because the coupling between the chains is comparable to the intrachain exchange, the spin system in $Cu_2V_2O_7$ is three dimensional from the standpoint of ESR. Thus the results of Refs. 39,46 might not be straightforwardly applicable. As it emerges from our experimental data the large DM interaction, amounting to at least $\sim 7\%$ of the isotropic exchange (see Sec. III A), present in α-$Cu_2V_2O_7$ has several consequences for the ESR spectrum. First, with $M_2 \approx |\mathbf{D}_{12}| \approx 0.07J$, Eq. (5) yields $\Delta H_{ex} \simeq 6$ kOe [Here $\mathbf{D}_{12}$ is the intrachain DM interaction as defined in Eq. (B2)]. Such a broad resonance line corresponds to a relaxation rate of the order of 2×10^{10} sec^{-1}, which is shorter than the frequency scale of the measurement. Obviously, this would explain the absence of an ESR response signal in the paramagnetic state of α-$Cu_2V_2O_7$. On the other hand, the result for a 1D-spin chain[39,46] $\Delta H \sim D^4/J^3$ yields a much smaller linewidth of the order of 20–30 Oe. Such a narrow resonance would be easily observable. Second, the occurrence of a ferromagneticlike signal in the AF ordered state of this compound can be attributed to the DM weak ferromagnetism. Usually, the observation of magnetic resonance in antiferromagnets requires electromagnetic fields in the millimeter wavelength or infrared region, or very strong static external fields. This is due to a large magnetocrystalline anisotropy energy and exchange energy as compared to the Zeeman energy. AF resonance at centimeter wave lengths (e.g., *X* band) is expected only in ''easy plane'' antiferromagnets which have a symmetry higher than rhombic.[9] In an antiferromagnet with a rhombic or lower symmetry with a DM interaction, however, the resonance frequency is of order $[J(A \pm D^2/J)]^{1/2}$. In this case the ''low'' frequency mode may fall into the *X* band due to a renormalization of some combination of usual anisotropy constants by the DM interaction resulting in small values of $A - D^2/J$.[9,10] Thus, the observation of magnetic resonance at $T < T_N$ in the low symmetry α-$Cu_2V_2O_7$ gives further support of the presence of the DM interaction.

Magnetic resonance of the β phase of $Cu_{2-y}Zn_yV_2O_7$ is entirely different. No resonance is observed in the ordered state, whereas a strong ESR signal appears above T_N. Because the Curie-Weiss temperature Θ in the two structural phases differs only moderately, the strength of the isotropic Heisenberg exchange should also remain comparable. Thus, the narrowing of the signal, as follows from Eq. (5), implies a significant reduction of the anisotropy of superexchange. As discussed in the previous section, the linewidth between 40 and 150 K is determined mainly by the spin-spin interactions in the paramagnetic regime. Hence, Eq. (5) can be used for the estimate of the second moment M_2, which is the measure of the anisotropic contribution to superexchange. With $\Delta H \approx 700$ Oe and $J = 72$ K one obtains $M_2 \sim 4\%$ of *J*. This anisotropy is therefore smaller than the DM interaction in the α phase. Since neither a ferromagnetic signal nor a spontaneous magnetization are found in the β phase, the reduction of the magnetic anisotropy suggests a strong change of DM interactions upon the structural transition. These conclusions agree well with the symmetry consideration made in Secs. IV A and IV B. Indeed, in the β phase the strongest intrachain interaction (B4) does not contain a D_{12}-antisymmetric DM interaction. A conventional estimate of the remaining symmetric nondiagonal deviations d_{12} [Eq. (B4)] from J_{12}-isotropic intrachain exchange in terms of the shift of the *g* factor from its spin-only value $\Delta g = g - 2$ yields $d_{12} \simeq (\Delta g/g)^2 J_{12} \approx 0.4\%$ of J_{12}.[7] This estimate is too small to explain the observed magnitude of the second moment M_2. The next contribution to M_2 can come from the D_{13}-antisymmetric part of the interchain interaction (B5), which can be related to the interchain isotropic exchange constant J_{13} [Eq. (B6)] as $D_{13} \simeq (\Delta g/g) J_{13}$.[7] With $J_{13} \sim 10$ K (see Sec. III A) one obtains D_{13} less than 1% of J_{12}. Thus, to account for the observed width of the ESR line in the β phase of $Cu_{2-y}Zn_yV_2O_7$ an enhancement of the *symmetric* anisotropic intrachain exchange in almost rectangular Cu-O bonds has to be taken into account.[12,13] In such bonding geometry one finds experimentally the symmetric anisotropic corrections up to 10% of the leading intrachain Heisenberg superexchange.[14,15]

V. CONCLUSIONS

We have studied the structural and magnetic properties of the spin-chain compound $Cu_{2-y}Zn_yV_2O_7$. We find that the substitution of nonmagnetic Zn for Cu leads to a structural transition from the α phase, found for $y < 0.15$, to the β phase, which occurs for $y \geqslant 0.15$. The local bonding geometry in the Cu-O chains changes due to this polymorphic transformation. Static magnetization and ESR data reveal a drastic difference in the magnetic properties of the two structural phases. In both cases the leading isotropic Heisenberg superexchange is aniferromagnetic and of similar strength and the weak interchain coupling leads to 3D antiferromagnetic order at low temperatures. The structural phase transition, however, affects strongly the anisotropic part of the spin-spin interaction. In the α phase the anisotropy is dominated by the Dzyaloshinsky-Moriya intrachain interaction, as suggested by the observation of a weak spontaneous magnetization and a ferromagneticlike resonance in the ordered state. In the β phase the anisotropy of the superexchange is strongly reduced. From our results and on the basis of a symmetry analysis taking account of the local bonding geometry we argue that the intrachain DM interaction is absent in the β phase. The remaining anisotropy in the β phase may be attributed to the symmetric anisotropic intrachain exchange in the almost rectangular Cu-O bond and the anisotropy of the interchain magnetic coupling.

ACKNOWLEDGMENTS

We acknowledge support by the Deutsche Forschungsgemeinschaft through SFB 608 and SPP 1073 and by NATO Collaborative Linkage Grant No. PST.CLG.977766 and INTAS Grant No. 01-0278. A.F. acknowledges support by the VolkswagenStiftung. V.K. acknowledges useful discussions with A. Möller.

APPENDIX A: GROUP THEORY ANALYSIS OF MAGNETIC STRUCTURE

In this analysis it is assumed that the magnetic order does not alter (e.g., double) the primitive cell of the crystal, i.e.,

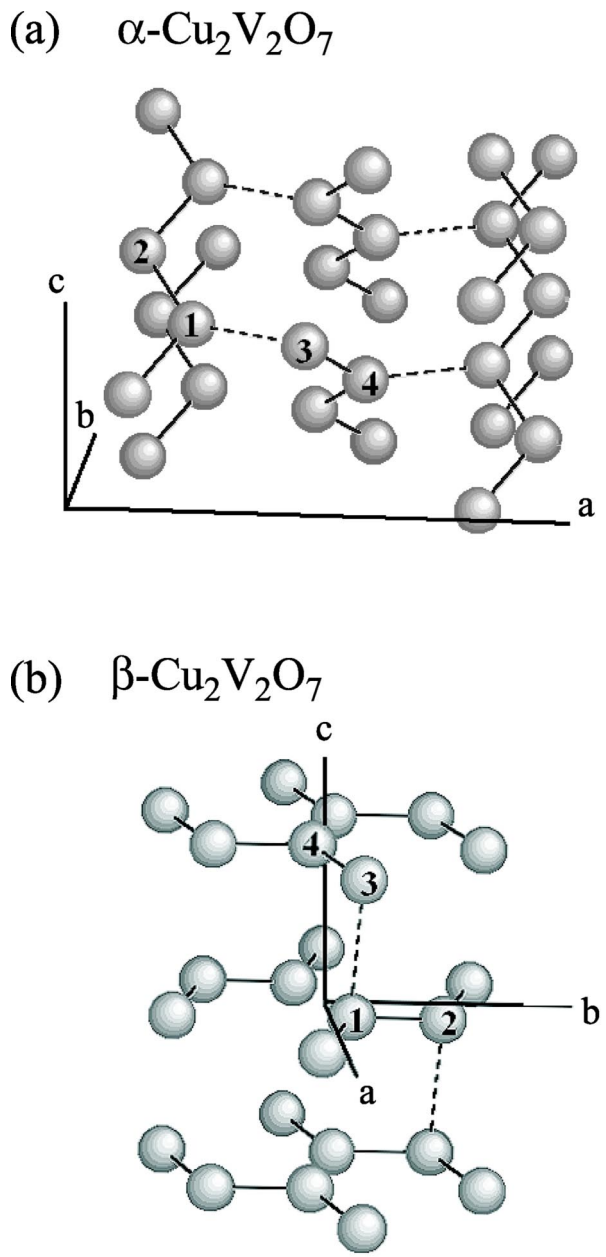

FIG. 9. (a) The choice of a primitive cell of the α phase of $Cu_2V_2O_7$. Only the Cu ions are shown, labeled from 1 to 4. Cu-site positions are (1) (0.165; 0.364; 3/4), (2) (0.085; 0.614; 1), (3) (0.335; 0.136; 3/4), (4) (0.415; 0.386; 1/2). The solid lines connect Cu ions in a chain with a distance 3.12 Å and the dashed lines mark the shortest interchain distance equal to 4 Å. (b) The choice of a primitive cell of the β phase of $Cu_2V_2O_7$. Cu-site positions are (1) (0.3098; 0.0736; 0.0140), (2) (0.1902; 0.4264; -0.0140), (3) (0.6902; 0.0736; 0.4860), (4) (0.3098; -0.0736; 0.5140). The distances between the ions labeled with 1–2 and 3–4 are equal to 2.95 and 3.26 Å, respectively. The dashed lines mark the shortest interchain distance equal to 4.64 Å.

that the magnetic cell coincides with the crystallographic cell. It is then sufficient to consider the symmetry of the magnetic moments of the Cu ions. We note that the four-sublattice model is a minimal model to describe magnetic ordering in two constrained AF chains running almost perpendicular to each other. The primitive cell of the α phase (space group $Fdd2$) contains four Cu ions in the $4b$ position while that of the β phase (space group $C2/c$) contains four Cu ions in the $4f$ position. The primitive cells and the coordination of the Cu ions are shown in Fig. 9. Note that the exchange interactions between the ions labeled 1 and 2 as well as 3 and 4 are intrachain interactions, while those between the ions 1 and 3 and 2 and 4 are the strongest interchain interactions.

TABLE I. Symmetry of magnetic modes in α-$Cu_2V_2O_7$.

$Fdd2$	e	2_z	σ_y	σ_x	
A_1	1	1	1	1	L_{1x}, L_{3y}, L_{2z}
A_2	1	1	−1	−1	L_{3x}, L_{1y}, F_z
B_1	1	−1	1	−1	L_{2x}, F_y, L_{1z}
B_2	1	−1	−1	1	F_x, L_{2y}, L_{3z}

Let us introduce magnetic modes as linear combinations of sublattice spins $\mathbf{S}_\alpha$, where α denotes a particular sublattice

$$\mathbf{F}=\mathbf{m}_1+\mathbf{m}_2,$$

$$\mathbf{L}_1=\mathbf{m}_1-\mathbf{m}_2,$$

$$\mathbf{L}_2=\mathbf{l}_1+\mathbf{l}_2,$$

$$\mathbf{L}_3=\mathbf{l}_1-\mathbf{l}_2. \tag{A1}$$

Here $\mathbf{l}_1=\mathbf{S}_1-\mathbf{S}_2$ and $\mathbf{l}_2=\mathbf{S}_3-\mathbf{S}_4$ denote AF vectors and $\mathbf{m}_1=\mathbf{S}_1+\mathbf{S}_2$ and $\mathbf{m}_2=\mathbf{S}_3+\mathbf{S}_4$ the sublattice magnetization. $\mathbf{F}$ is the ''ferromagnetism vector'' of the crystal. $\mathbf{L}_1$ is determined by the difference of the ferromagnetism vectors of neighboring chains. $\mathbf{L}_2$ and $\mathbf{L}_3$ represent the intrachain AF ordering. For a second order magnetic phase transition the possible magnetic structures can be classified by the irreducible representations of the symmetry group of the crystal in paramagnetic phase.[44] The results of the symmetry operations are summarized in Tables I and II for the α and the β phase, respectively. In each table the first column contains irreducible representations of a respective space group; corresponding symmetry operations and basis vectors of magnetic structure are listed in the second and the third column, respectively. For rhombic Heisenberg magnets only one basis vector describes the magnetic structure in exchange approximation since the leading isotropic exchange is much stronger than DM and anisotropic interactions. In our case the average magnitude of such a vector in the ordered state will be close to $4\langle S\rangle$ while the other ones belonging to the same irreducible representation will be smaller by order of D/J.

TABLE II. Symmetry of magnetic modes in β-$Cu_2V_2O_7$.

$C2/c$	e	2_y	I	σ_y	
A_g	1	1	1	1	L_{1x}, F_y, L_{1z}
A_u	1	1	−1	−1	L_{3x}, L_{2y}, L_{3z}
B_g	1	−1	1	−1	F_x, L_{1y}, F_z
B_u	1	−1	−1	1	L_{2x}, L_{3y}, L_{2z}

In the α phase in three of the irreducible representations the ferromagnetism vector **F** coexists with $\mathbf{L}_2$ or $\mathbf{L}_3$ vectors, which represent uniform AF ordering on the chain. Thus antiferromagnetic order with canted moments and resulting weak ferromagnetism is possible. Only one irreducible representation (A_1) does not contain any component of the ferromagnetic vector. However, such canted magnetic structure without weak ferromagnetic moment must consist of more than two spins which we really deal with. As is apparent from Table II, components of the $\mathbf{L}_2$ and $\mathbf{L}_3$ vectors and the ferromagnetism vector **F** do not coexist in the same irreducible representation in the β phase. This implies that in the β-phase weak ferromagnetism is incompatible with AF ordering in the chains.

APPENDIX B: EXCHANGE INTERACTION TENSORS

Generally, the nondiagonal components of the exchange interaction tensor [Eq. (4)] can be split into antisymmetric and symmetric parts

$$K^{Aij}_{\alpha\beta}=\tfrac{1}{2}\,(K^{ij}_{\alpha\beta}-K^{ji}_{\alpha\beta})=D^{l}_{\alpha\beta}e_{lij}\,,$$

$$K^{Sij}_{\alpha\beta}=\tfrac{1}{2}\,(K^{ij}_{\alpha\beta}+K^{ji}_{\alpha\beta})=d^{l}_{\alpha\beta}|e_{lij}|, \tag{B1}$$

respectively, where e_{lij} is the totally antisymmetric tensor. Note that for the given symmetries of the α and β phases the nondiagonal components of the intrachain and interchain interactions can be either purely antisymmetric or purely symmetric. The antisymmetric part is usually represented as the components of the Dzyaloshinskii-Moriya vector **D**.

Let us consider the orientation of the DM vector for intrachain-K^{ij}_{12} and interchain-K^{ij}_{13} interactions. For the α phase the symmetry analysis yields

$$K^{ij}_{12}=\begin{pmatrix} K^{xx}_{12} & D^{z}_{12} & D^{y}_{12} \\ -D^{z}_{12} & K^{yy}_{12} & d^{x}_{12} \\ -D^{y}_{12} & d^{x}_{12} & K^{zz}_{12} \end{pmatrix} \tag{B2}$$

and

$$K^{ij}_{13}=\begin{pmatrix} K^{xx}_{13} & d^{z}_{13} & D^{y}_{13} \\ d^{z}_{13} & K^{yy}_{13} & D^{x}_{13} \\ -D^{y}_{13} & -D^{x}_{13} & K^{zz}_{13} \end{pmatrix}. \tag{B3}$$

Equations (B2) and (B3) show that the antisymmetric intrachain interaction between ions 1 and 2 (Fig. 9) gives rise to a DM vector with *y* and *z* components, whereas the antisymmetric interchain interaction between ions 1 and 3 gives rise to a DM vector with *x* and *y* components.

For the β phase we obtain

$$K^{ij}_{12}=\begin{pmatrix} K^{xx}_{12} & d^{z}_{12} & d^{y}_{12} \\ d^{z}_{12} & K^{yy}_{12} & d^{x}_{12} \\ d^{y}_{12} & d^{x}_{12} & K^{zz}_{12} \end{pmatrix} \tag{B4}$$

and

$$K^{ij}_{13}=\begin{pmatrix} K^{xx}_{13} & D^{z}_{13} & d^{y}_{13} \\ -D^{z}_{13} & K^{yy}_{13} & D^{x}_{13} \\ d^{y}_{13} & -D^{x}_{13} & K^{zz}_{13} \end{pmatrix}. \tag{B5}$$

Apparently, weak ferromagnetism is incompatible with AF ordering in the chains. K^{ij}_{12} contains no antisymmetric components, whereas small symmetric nondiagonal components in K^{ij}_{12} and antisymmetric components of K^{ij}_{13} lead to the small canting of the four-sublattice spin structure without the appearance of a weak ferromagnetic moment.

Using the above results we rewrite the isotropic (Heisenberg) part of Hamiltonian Eq. (4) in an invariant form

$$\mathcal{H}_{ex}=\tfrac{1}{4}\,[(J_{11}+J_{12}+J_{13}+J_{14})\mathbf{F^2}+(J_{11}+J_{12}-J_{13}-J_{14})\mathbf{L_1^2} +(J_{11}-J_{12}+J_{13}-J_{14})\mathbf{L_2^2}+(J_{11}-J_{12}-J_{13}+J_{14})\mathbf{L_3^2}], \tag{B6}$$

where the magnetic modes **F**, $\mathbf{L}_1$, $\mathbf{L}_2$, and $\mathbf{L}_3$ are defined in Eq. (A1). This form is the same for the α and β phases. AF ordering in the chains occurs when $J_{12}>0$. Note that $J_{12}=J_{34}=2J$ in the α phase and $J_{12}=J_{34}=J+J'$ (see Sec. IV A) in the β phase in the nearest-neighbor approximation. Since $J_{14}\ll J_{13}$, the mutual orientation of the AF vectors of neighboring chains depends on the sign of the interchain exchange $J_{13}(=J_{24})$. The ferromagnetic interchain exchange $J_{13}<0$ favors $\mathbf{L}_2$-type magnetic ordering with parallel $\mathbf{l}_1$ and $\mathbf{l}_2$ vectors. In contrast, the AF interchain exchange $J_{13}>0$ stabilizes antiparallel ordering of $\mathbf{L}_3$ type.

*Present address: Max Planck Institute for Solid State Research, MPI-FKF, 70569 Stuttgart, Germany.

[1] G. Grüner, *Density Waves in Solids*, Vol. 89 of *Frontiers in Physics Series* (Addison-Wesley, New York, 1994).
[2] T. Lorenz, M. Hofmann, M. Grüninger, A. Freimuth, G. S. Uhrig, M. Dumm, and M. Dressel, Nature (London) **418**, 614 (2002).
[3] M. Hase, I. Terasaki, and K. Uchinokura, Phys. Rev. Lett. **70**, 3651 (1993).
[4] M. Uehara, T. Nagata, J. Akimitsu, H. Takahashi, N. Môri, and K. Kinoshita, J. Phys. Soc. Jpn. **65**, 2764 (1996).
[5] T. Nagata, M. Uehara, J. Goto, J. Akimitsu, N. Motoyama, H. Eisaki, S. Uchida, H. Takahashi, T. Nakanishi, and N. Môri., Phys. Rev. Lett. **81**, 1090 (1998).
[6] I. Dzyaloshinsky, Phys. Chem. Solids **4**, 241 (1958).
[7] T. Moriya, Phys. Rev. **120**, 91 (1960).
[8] J. B. Goodenough, Phys. Rev. **100**, 564 (1955); J. Kanamori, J. Phys. Chem. Solids **10**, 87 (1959); P. W. Anderson, Solid State Phys. **14**, 99 (1963).
[9] E. A. Turov, *Physical Properties of Magnetically Ordered Crystals* (Academic Press, New York, 1965).
[10] T. A. Kaplan, Z. Phys. B: Condens. Matter **49**, 313 (1983); L. Shekhtman, O. Entin-Wohlman, and A. Aharony, Phys. Rev. Lett. **69**, 836 (1992); A. Zheludev, S. Maslov, I. Tsukada, I. Zaliznyak, L. P. Regnault, T. Masuda, K. Uchinokura, R. Erwin, and G. Shirane, *ibid.* **81**, 5410 (1998).

[11] I. Tsukada, J. Takeya, T. Masuda, and K. Uchinokura, Phys. Rev. Lett. **87**, 127203 (2001).
[12] V. Yushankhai and R. Hayn, Europhys. Lett. **47**, 116 (1999).
[13] S. Tornow, O. Entin-Wohlman, and A. Aharony, Phys. Rev. B **60**, 10 206 (1999).
[14] V. Kataev, K.-Y. Choi, M. Grüninger, U. Ammerahl, B. Büchner, A. Freimuth, and A. Revcolevschi, Phys. Rev. Lett. **86**, 2882 (2001).
[15] H.-A. Krug von Nidda, L. E. Svistov, M. V. Eremin, R. M. Eremina, V. Kataev, A. Loidl, A. Prokofiev, and W. Assmus, Phys. Rev. B **65**, 134445 (2002).
[16] D. Mercurio-Lavaud and B. Rit, Acta Crystallogr., Sect. B: Struct. Crystallogr. Cryst. Chem. **29**, 2731 (1973).
[17] C. Calvo and R. Faggiani, Acta Crystallogr., Sect. B: Struct. Crystallogr. Cryst. Chem. **31**, 603 (1975).
[18] D. Mercurio-Lavaud and B. Frit, C. R. Seances Acad. Sci., Ser. C **277**, 1101 (1973).
[19] P. Fleury, C. R. Seances Acad. Sci., Ser. C **263**, 1375 (1966); P. Fleury, Rev. Chim. Miner. **6**, 819 (1969).
[20] J. Pommer, Ph.D. thesis, Aachen Technical University, 2002.
[21] L. A. Ponomarenko, A. N. Vasil'ev, E. V. Antipov, and Yu. A. Velikodny, Physica B **284-288**, 1459 (2000).
[22] M. A. Kastner, R. J. Birgeneau, G. Shirane, and Y. Endoh, Rev. Mod. Phys. **70**, 897 (1998), and references therein.
[23] J. C. Bonner and M. E. Fischer, Phys. Rev. **135**, A640 (1964).
[24] W. E. Hatfield, J. Appl. Phys. **52**, 1985 (1981).
[25] A. M. Finkelstein, V. E. Kataev, E. F. Kukovitskii, and G. B. Teitelbaum, Physica C **168**, 370 (1990); G. Xiao, M. Z. Cieplak, J. Q. Xiao, and C. L. Chien, Phys. Rev. B **42**, 8752 (1990); G. Khaliullin, R. Kilian, S. Krivenko, and P. Fulde, *ibid.* **56**, 11 882 (1997).
[26] In almost insulating La_2CuO_4 the Zn-induced moments are correlated, however, rather strongly at $T > T_N$, owing to a very large magnetic correlation length in the CuO_2 planes in the paramagnetic state, and order three dimensionally at T_N (see, M. Hücker and B. Büchner, Phys. Rev. B **65**, 214408 (2002)].
[27] In the fits of the susceptibility data for $y < 0.15$ to the Curie-Weiss law a temperature independent term χ_0 was neglected, because it could not be determined unambiguously from the fit. If one takes $\chi_0 = 1 \times 10^{-4}$ emu/mole Cu, as determined for the samples with $y \geqslant 0.15$, the values of Θ get somewhat smaller, as compared with the results shown in Fig. 5. This does not affect, however, the conclusions of our qualitative discussion.
[28] A. N. Vasil'ev, L. A. Ponomarenko, A. I. Smirnov, E. V. Antipov, Yu. A. Velikodny, M. Isobe, and Y. Ueda, Phys. Rev. B **60**, 3021 (1999).
[29] H. J. Schulz, Phys. Rev. Lett. **77**, 2790 (1996).
[30] T. Oguchi, Phys. Rev. **133**, A1098 (1964); T. Ishikawa and T. Oguchi, Prog. Theor. Phys. **54**, 1282 (1975).
[31] M. J. Hennessy, C. D. McElwee, and P. M. Richards, Phys. Rev. B **7**, 930 (1973).
[32] Resonance signals at low frequencies in a canted antiferromagnet have been studied, e.g., in hematite $\alpha - Fe_2O_3$ (Ref. 33). We note that the shape and position of the signal in a polycrystalline sample depends on the relative strength of the external field H and on the magnetization of individual grains, which is distributed randomly around the direction of H.
[33] H. Kumagai, H. Abe, K. Ôno, I. Hayashi, J. Shimada, and K. Iwanaga, Phys. Rev. **99**, 1116 (1955); P. Pincus, Phys. Rev. Lett. **5**, 13 (1960).
[34] A. Abragam and B. Bleaney, *Electron Paramagnetic Resonance of Transition Ions* (Clarendon, Oxford, 1970).
[35] To estimate the anisotropy of the g factor we mixed the fine powder of $y = 0.2$ sample with epoxy glue and let the mixture harden in a magnetic field of 1 T. Owing to the anisotropy of the g factor the powder particles are oriented by the field so that the sample acquires a uniaxial magnetic anisotropy axis. The so prepared sample exhibits at room temperature an anisotropic ESR signal with $g_\parallel = 2.23$ and $g_\perp = 2.09$ for **H** parallel and perpendicular the direction of this axis, respectively. These values are typical for a Cu^{2+} ion with a single hole $S = 1/2$ in the $d_{x^2-y^2}$ orbital (Ref. 34). The average g factor $g = \sqrt{(1/3)g_\parallel^2 + (2/3)g_\perp^2} = 2.14$ is close to the mean value obtained for the nonoriented powder and $(g_\parallel - g_\perp)/g \simeq 7\%$.
[36] D. L. Huber, Phys. Rev. B **6**, 3180 (1972).
[37] H. Benner and J. P. Boucher, in *Magnetic Properties of Layered Transition Metal Compounds*, edited by L. J. de Jongh (Kluwer Academic, Dordrecht, 1990), p. 323.
[38] The theory in Ref. 39 predicts that at sufficiently low temperatures $T \ll J$ but still well above any three-dimensional ordering the ESR signal in a 1D spin chain broadens as $1/T^2$ due to fluctuating staggered field caused by the DM interaction or staggered g tensor. Apparently this theory cannot be related to the low-temperature broadening of the signal in β-$Cu_2V_2O_7$ as it occurs only close to T_N (see also Sec. IV C).
[39] M. Oshikawa and I. Affleck, Phys. Rev. Lett. **82**, 5136 (1999); Phys. Rev. B **65**, 134410 (2002).
[40] M. Schindler and F. C. Hawthorne, J. Solid State Chem. **146**, 271 (1999).
[41] $d_{x^2-y^2}$ is the ground state orbital of Cu^{2+} in the β phase, as is evident from the value of the g factor (Ref. 35). We assume that it remains the ground state orbital in the α phase also, owing to the similar symmetries of the CuO_5 polyhedra in the two phases. The occurrence of the $d_{x^2-y^2}$ ground state in both phases is predicted by the angular overlap model (Ref. 42).
[42] A. Möller (private communication).
[43] E. F. Bertaut, Acta Crystallogr., Sect. A: Cryst. Phys., Diffr., Theor. Gen. Crystallogr. **24**, 217 (1968); E. F. Bertaut, J. Phys. (France) **32**, 462 (1971); E. F. Bertaut, J. Magn. Magn. Mater. **24**, 267 (1981).
[44] Yu. A. Izyumov and V. E. Naish, J. Magn. Magn. Mater. **12**, 239 (1979).
[45] R. Kubo and K. Tomita, J. Phys. Soc. Jpn. **9**, 888 (1954).
[46] J. Choukroun, J.-L. Richard, and A. Stepanov, Phys. Rev. Lett. **87**, 127207 (2001).